This is the peer-reviewed, final accepted version for American Mineralogist, published by the Mineralogical Society of America.
The published version is subject to change. Cite as Authors (Year) Title. American Mineralogist, in press.
DOI: https://doi.org/10.2138/am-2021-7851. http://www.minsocam.org/

Revision #1

The atomic arrangement and electronic interactions in vonsenite at 295, 100, and 90 K

MARC MADERAZZO[1,ξ], JOHN M. HUGHES[1,2], M. DARBY DYAR[3], GEORGE R. ROSSMAN[4], BRANDON J. ACKLEY[5], ELIZABETH C. SKLUTE[3], MARIAN V. LUPULESCU[6], AND JEFFREY CHIARENZELLI[7]

[1]Department of Geology, University of Vermont, Burlington, Vermont, 05405, U.S.A.
[2]Department of Geology and Environmental Earth Sciences, Miami University, Oxford, Ohio 45056, U.S.A.
[3]Department of Astronomy, Mount Holyoke College, South Hadley, Massachusetts 01075, U.S.A.
[4]Division of Geological and Planetary Sciences, California Institute of Technology, Pasadena, California 91125-2500, U.S.A.
[5]Department of Chemistry, University of Vermont, Burlington, Vermont, 05405, U.S.A.
[6]New York State Museum, Research and Collections, 3140 CEC, Albany, New York 12230, U.S.A.
[7]Department of Geology, St. Lawrence University, Canton, New York 13617, U.S.A.

ABSTRACT

Vonsenite, $Fe^{2+}_2Fe^{3+}O_2BO_3$, has been the subject of many studies in the materials-science and condensed-matter-physics communities due to interest in the electronic and magnetic properties and ordering behavior of the phase. One such study, undertaken on synthetic material of endmember composition, reports X-ray diffraction structure refinements that indicate a phase transition from *Pbam* to *Pbnm* at or just below approximately 283 K, determined subsequently to arise from a Peierls-like instability. To compare the stability of the natural phase with that of synthetic material, we performed high-precision X-ray crystal structure analyses at 295, 100, and 90 K (R_1 = 0.0119, 0.0186, and 0.0183, respectively), Mössbauer spectroscopy at 295, 220, 150, 80, and 4.2 K, and wavelength-dispersive electron microprobe analysis on a vonsenite of near-

ξ E-mail: marc.maderazzo@uvm.edu

endmember composition from Jayville, New York, U.S.A. The *Pbnm* structure is observed at 100 K and 90 K, suggesting similar phase stability for the natural and synthetic phases. Comparison of Mössbauer data and X-ray site occupancies between the natural and synthetic phases suggests a reinterpretation of Mössbauer site assignments. We conclude that the Peierls-like instability underlying the reported transition from *Pbam* to *Pbnm* in synthetic material occurs also in our specimen of natural near-endmember vonsenite at temperatures between 295 K and 100 K.

Keywords: vonsenite, phase transition, low-temperature structure refinements, Peierls-like instability

INTRODUCTION

Vonsenite, $Fe^{2+}_2Fe^{3+}O_2BO_3$, is the heterovalent-iron endmember of the ludwigite group of high-temperature contact-metamorphic oxyborates. Vonsenite forms a continuous isomorphic solid-solution series with ludwigite *sensu stricto*, $Mg_2Fe^{3+}O_2BO_3$ (Tschermak 1874). The ludwigite group minerals are common accessories in boron-rich magnesian and calcareous iron skarns after dolomites (Palache et al. 1951). Vonsenite is much less common than ludwigite.

Takéuchi et al. (1950) first determined the structure of a natural ludwigite, and Takéuchi (1956) refined the structure of a natural magnesian vonsenite ($Fe^{2+}_{0.625}Mg_{0.375}$) using Weissenberg data. Mokoyeva (1968) refined the structure of two crystals of synthetic ludwigite, $[(Mg_{1.85}Fe^{2+}_{0.15})(Fe^{3+}_{0.60}Al_{0.40}]BO_3O_2$, and was first to report the distribution of Fe^{2+} and Fe^{3+} over the cation sites. Swinnea and Steinfink (1983) refined the structure of a crystal of synthetic endmember vonsenite, supporting many prior findings and surpassing earlier structure refinements by an order of magnitude in precision. Structure refinement was attained to R = 0.030, in space group *Pbam*; the atom nomenclature of those authors is generally respected in

later investigations, and we continue that practice in this work. Based on Mössbauer spectra, site distortions, and bond valence sums, the authors report that Fe^{2+} occupies Fe1 and Fe3. "Direct exchange" is reported between Fe2 and Fe4 [separated by 2.783 Å at 295 K (Table 3), "direct exchange" is understood here to mean intervalence charge transfer, after the cited Burns (1981), though the authors do not express this claim categorically], resulting in an intermediate valence of $Fe^{2.5+}$ on both sites. Significantly, Mössbauer spectra are reported to establish the presence of charge delocalization along [001] as a function of temperature.

The pivotal work of Swinnea and Steinfink (1983) set the stage for many studies of vonsenite structure, crystal chemistry, and electronic interactions by the materials-science and condensed-matter-physics communities. These studies were undertaken to explore and understand the subtle, complex electronic and magnetic characteristics of the phase, its ordering behavior, and its manifestation of multiferroicity [see van den Brink and Khomskii (2008) for a technical introduction to multiferroicity; Maignan et al. (2017) assume familiarity with multiferroicity and discuss it specifically in vonsenite]. All such studies known to the present authors [cf. the exhaustive review of Sofronova and Nazarenko (2017)] were performed upon synthetic vonsenite powders and single crystals of ideal endmember composition, prepared by a variety of synthesis techniques.

Although the atomic arrangement of synthetic vonsenite has been studied extensively, there is a paucity of structure studies on natural vonsenite, and, to our knowledge, natural materials have not been studied at lower-than-ambient temperatures. Notably, Bonazzi and Menchetti (1989) refined the structures of three natural vonsenites in a broader study of ludwigite crystal chemistry, confirming *Pbam* isomorphism throughout the solid solution at STP (IUPAC Standard Temperature and Pressure = 273.15 K, 100 kPa = 1 Bar).

Subsequent to the initial investigations of the vonsenite atomic arrangement at STP, Bordet and Suard (2009) performed X-ray structure refinements upon a single crystal of synthetic endmember vonsenite at temperatures between 320 K and 110 K and reported a structural transition from *Pbam* to *Pbnm* at or just below 283 K. That transition, and the magnetic properties and magnetic transitions of the *Pbnm* structural phase at lower temperatures, have been the subject of numerous studies in the materials-science and condensed-matter-physics communities. Biryukov et al. (2020) refined the structure of a natural vonsenite at 293 K (R = 0.036) and 400 K, (R = 0.029). The paper examines and compares the variation of oxidation states and the associated structural changes in a natural near-endmember vonsenite and a compositionally similar hulsite from the same occurrence, and the solid-state decomposition of hulsite to warwickite plus hematite.

The atomic arrangement of vonsenite at 295 K is depicted in Figure 1. Fe cations occupy four octahedra, Fe1–Fe4, which are corner- and edge-shared in (001). The four sites may be associated in symmetrically nonequivalent pairs: Fe1 with Fe3, and Fe2 with Fe4. Fe1 (2*a;* site symmetry 2/*m*) and Fe3 (4*g*; site symmetry *m*) exhibit distinctly longer Fe-O distances in the equatorial plane, whereas Fe2 (2*d*; site symmetry 2/*m*) and especially Fe4 (4*h*; site symmetry *m*) are highly symmetric. Fe1 and Fe3 lie in the $z = 0$ plane; Fe2 and Fe4 lie at $z = 1/2$.

The FeO_6-octahedra form zigzag chains on (001). Within each zigzag chain, edge-shared three-member subsequences (Fe4-Fe1-Fe4) and (Fe3-Fe2-Fe3) recur in the unbounded continuous sequence $(Fe4\text{-}Fe1\text{-}Fe4\text{-}Fe3\text{-}Fe2\text{-}Fe3)_{\infty}$. Zigzag chains are linked in (001) by corner-sharing, creating interstices for triangular BO_3 groups in which each vertex is an equatorial oxygen shared by two FeO_6-octahedra (Fig. 1).

This is the peer-reviewed, final accepted version for American Mineralogist, published by the Mineralogical Society of America.
The published version is subject to change. Cite as Authors (Year) Title. American Mineralogist, in press.
DOI: https://doi.org/10.2138/am-2021-7851. http://www.minsocam.org/

FeO_6-octahedra also comprise structural elements termed triads (Sofranova and Nazarenko 2017), which are of two types. Sites Fe2 and Fe4 form edge-shared 4-2-4 triads in (001), termed triads of the first type (orange octahedra in Fig. 1); sites Fe1 and Fe3 form corner-shared 3-1-3 triads of the second type (yellow octahedra in Fig. 1). Both triad types stack along [001], sharing edges between adjacent unit cells ($c \sim 3.07$ Å, i.e., a single octahedron) to form zigzag walls (Guimarães et al. 1999). Zigzag walls are quasi-two-dimensional structures within which correlated electronic interactions induce the singular electronic, magnetic, transport, and ordering behavior observed in studies of synthetic material.

We report high-quality structure refinements from data collected at 295 K, 100 K, and 90 K on a ground, spherical single crystal of a natural vonsenite, $(Fe^{2+}_{1.90}Mg_{0.08}Mn^{2+}_{0.02})_{\Sigma 2.00}(Fe^{3+}_{0.98}Al_{0.02})_{\Sigma 1.00}BO_5$, from Jayville, New York, U.S.A., and provide a concise summary of the structures.

EXPERIMENTAL

Chemical Analysis. A 5 mm vonsenite crystal from the current locality was mounted in epoxy in a 1-inch ring, polished, carbon coated under vacuum and analyzed by wavelength-dispersive X-ray spectrometry using a Cameca SX-100 electron-probe at the Earth and Environmental Sciences Department, Rensselaer Polytechnic Institute, Troy, NY. Operating conditions were 15 keV and 20 nA. The standards used were kyanite (Al), hematite (Fe), tephroite (Mn), rutile (Ti), synthetic V_2O_5 (V), chromite (Cr). The results of the analyses are given in Table 1[1].

X-ray Diffraction. X-ray diffraction data were collected with a Bruker ApexII CCD single-crystal diffractometer using graphite-monochromated Mo K_α radiation; details of crystal data and data collection are contained in a single CIF (Crystallographic Information File) for the

three structures; that file has been deposited.[1] Temperature was controlled using an Oxford Cryostream Controller 700 paired with an Oxford Cryostream AD51 Dry Air Unit. The air stream is controlled using a Cryostream Cooler Nitrogen Gas Pump Unit. Actual temperatures (K) of data collection were 295.0(1.0) [henceforth 295], 100.5(1.0) [henceforth 100], and 90.5(1.0) [henceforth 90].

For each sample, redundant data were collected for a sphere of reciprocal space (average redundancy ≈ 9.6) and were integrated and corrected for Lorentz and polarization factors and absorption using the Bruker Apex2 package of programs. For the 295 K structure, the atomic arrangement was refined in space group *Pbam* with SHELXL-97 (Sheldrick 2008) using neutral atom scattering factors and full-matrix least-squares, minimizing the function $\Sigma w(F_o^2 - F_c^2)^2$ with no restraints. All atoms were refined with anisotropic temperature factors; an extinction coefficient was also refined. After completion of final refinements, the ferric/ferrous ratios were determined for each site (Table 2). For the 295 K structure, the small amount of substituent Mg (0.17apfu) was modeled, but not for the low-temperature structures. Experiments demonstrated that Fe2 and Fe4 refined within 1.5 esd of 26 electrons when the site occupancies were singly released in the three structures, whereas Fe1 refined to an average of 25.27 electrons and Fe3 refined to 25.18 electrons. Thus, the substituent Mg was modeled on Fe1 and Fe3.

The low-temperature superstructure in vonsenite is subtle but identifiable. For the 100 and 90 K structures, a weak superstructure which doubled the *c*-axis length was found only by

[1] Deposit item AM-19-xx1 contains Tables 1, 4a, 4b, 5a, 5b, and CIF files for the three structures reported herein. Deposit items are available two ways: for paper copies contact the Business Office of the Mineralogical Society of America (see inside front cover of recent issue) for price information. For an electronic copy visit the MSA web site at http://www.minsocam.org, go to the *American Mineralogist* Contents, find the table of contents for the specific volume/issue wanted, and then click on the deposit link there.

examining reflections with $I/\sigma_I < 10$. Those structures were successfully refined in space group *Pbnm* (non-standard setting of *Pnma,* chosen for axial comparison with the room-T *Pbam* structure), in accord with the space group found in earlier studies using synthetic material. To confirm that the superstructure is not observed at room temperature we reduced the reflection threshold to $I/\sigma_I = 2$ for cell determination. The putative room-temperature cell was confirmed.

In the *Pbnm* structures observed at 100 K and 90 K, there is evidence for site-splitting of the Fe2 site; a distinct peak in the difference map, the largest of the observed difference peaks, was found at ~ 0.27Å from the Fe2 site. This site-splitting is observed in both of the low-T refinements, and was refined in those structures. This local site splitting is distinct from the larger splitting of atomic sites due to the symmetry changes that result from the phase change described below.

Atomic coordinates and anisotropic displacement parameters for all atoms in vonsenite are contained in the deposited CIF, as well as selected interatomic distances including Fe-O distances that are germane to the subsequent discussion. Ferric/ferrous ratios for each of those sites are reported in Table 2 [determined using program *VaList*, Wills (2020)]. Table 3 contains selected Fe-Fe distances.

Mössbauer analysis. Mössbauer measurements were taken at 295, 220, 150, 80, and 4.2 K on a WEB Research (now SEE Co) W100 spectrometer using a ~100-80 mCi ^{57}Co source in Rh. Low-temperature spectra were obtained using a Janis Research Model 850 4K closed-cycle helium compression system that allows for temperature control from 300 K to 4.2 K (±1 K). Run times ranged from 6 to 48 hours. All spectral baselines were corrected for Compton scattering of the 122 keV gamma rays. Spectra were collected in 1024 channels. Each spectrum was folded, corrected for nonlinearity, and interpolated to a linear velocity scale using the program WMOSS

and a room-temperature 28-mm α-Fe foil calibration standard. Table 4a contains Mössbauer parameters for vonsenite, and Table 4b contains supplementary Mössbauer parameters for the phase. Table 5(a, b) provides a comparison of site assignments from the literature and this study; these four tables have been deposited.

Mössbauer spectra were fit using the Mex disdd program (de Grave and van Alboom 1991). Mex disdd solves the full hyperfine interaction Hamiltonian for multiple distributions, and minimizes the chi-squared deviation between the fitted and experimental spectrum using center shift (CS), quadrupole shift (QS), full width at half maximum, hyperfine field, distribution area, and asymmetry and angle parameters (relating to the electric field gradient, EFG) as free parameters.

RESULTS

The natural vonsenite specimen of the present work exhibited space group *Pbam* (No. 55) at 295 K, and space group *Pbnm* (No. 62) at 100 K and 90 K, consistent with the reported observations of Bordet and Suard (2009) on synthetic endmember material. The refinements on the natural material yielded the lowest *R* values reported to date for the room-T or low-T phases, either natural or synthetic.

The atomic arrangements of the dimorphs have been described using structures determined on synthetic material; here we forego a detailed structure description but briefly summarize the description of the ~283K phase transition provided by Bordet and Suard (2009). That phase transition, captured in the present work, is a consequence of electronic interactions discussed in detail below.

As reported by Bordet and Suard (2009), a principal structural consequence of the phase transition captured in the present work is the splitting of specific atomic positions into two

positions no longer related by symmetry. Among the Fe atoms, only Fe4 undergoes this splitting, whereas Fe1-Fe3 remain single sites but double their rank. Figure 2 illustrates the relationship, discussed in detail below, of the single *Pbam* Fe4 site to the two non-equivalent sites, Fe4a and Fe4b, in the *Pbnm* dimorph.

Additional atoms that undergo site-splitting in the phase transition are B, O1, O3, and O5, as noted in the CIFs. Although observable, these displacements are subtle; all shifts in atomic coordinates between split atoms that are symmetry equivalents in *Pbam* but are not in *Pbnm* are in the third decimal place, the largest being 0.007.

Of particular interest in the vonsenite atomic arrangements are the loci of ferrous and ferric iron atoms in the *Pbam* and *Pbnm* phases. From the structure refinements, Fe1 and Fe3 are occupied primarily by Fe^{2+} (Table 2), whereas Fe2 and Fe4 are occupied by Fe of intermediate valence. The largest variation in the low-temperature *Pbnm* phases is between the two sites that are split from the room-temperature, *Pbam*, Fe4 sites, renamed Fe4a and Fe4b sites in the *Pbnm* structure (Table 2).

Fe-O bond lengths for the four FeO_6-octahedra are contained in the CIFs. Fe-Fe distances germane to the electronic interactions in the vonsenite structures are contained in Table 3; observed changes in Fe-Fe distances and site valences arise from the electronic interactions described below. Note that for the 100K data, the atomic displacement parameters for Fe2 and Fe2', constrained to be equivalent, were slightly non-positive definite, and the same atoms refined with the 90K data were nearly non-positive definite. Such a situation is not uncommon for two such close split sites, and the anisotropic refinement was retained rather than converting the two atoms to isotropic refinement.

Mössbauer analysis. The Mössbauer spectra of mixed-valence compounds have been

studied extensively (Xuemin et al. 1984, Li et al. 1994, Mitov et al. 1999, Cherkezova-Zheleva et al. 2006). The study most similar to the present work is that of Douvalis et al. (2002), who characterized the electronic behavior of Fe_3BO_5 from 4.2 K to 620 K in considerable detail. The authors reverse the generally accepted definitions, after Swinnea and Steinfink (1983), for the Fe3 and Fe4 sites. In the subsequent discussion we compare their results with our own, revising their nomenclature to be consistent with the accepted usage.

Douvalis et al. (2002) report Mössbauer parameters that include averages of Fe^{2+} and Fe^{3+} contributions for the Fe2 and Fe4 sites, arising from electron delocalization due to the close proximity of the cations: 2.783 Å at 295 K (Table 3). Fe-Fe distances for other pairings of Fe-sites are ≥ 3.07 Å; without exception, no delocalization is observed. They also report evidence of complex magnetic transitions between 114 and 40 K, involving some or all Fe atoms, as suggested by Douvalis et al. (1997) and reported by Guimarães et al. (1999).

The Douvalis et al. (2002) assignments of Mössbauer doublet splittings are generally inconsistent with the site occupancies we observed, based on Mössbauer spectra taken at 295, 220, 150, 80, and 4.2 K (Figs. 3 and 4; see Appendix 1), and reconciled with our X-ray single-crystal structure refinement (SREF) data. To compare Mössbauer doublet assignments with site occupancies determined by structure refinement, we recast the data as percentages of total Fe (these data appear in the rightmost two columns of Table 5b, on deposit). Douvalis et al. (2002) assign the D1 doublet to Fe1, overfilling the site; we distribute the doublet between Fe1 and Fe3 sites, which are observed to be preferred by divalent cations. Similarly, the authors assign their D2 doublet to Fe4. The doublet area is too large to be solely Fe4, and likely is shared by Fe4 and Fe2. Their D3 doublet, primarily Fe^{3+}, was distributed between Fe2 and Fe3, but SREF finds Fe^{3+} in all four sites, suggesting that the authors' assignment is an oversimplification: there is no

a priori way to assign a distribution of delocalized charges to a specific site or to an arbitrary subset of all sites.

Tables 4a and 5 give assignments that reconcile observed Mössbauer spectral features with SREF results in the present work. Table 5a presents SREF site occupancies recast to doublet areas for the 90K Fe^{2+} and Fe^{3+} features, with the Fe in D4 and D5 split between Fe^{2+} and Fe^{3+}. Table 5b shows calculations and resultant values assigning these doublets to specific sites that agree most closely with SREF results.

ELECTRONIC INTERACTIONS, CORRELATIONS, AND STRUCTURE IN VONSENITE AT 295, 100, AND 90 K

Electrons in crystalline materials exhibit behaviors ranging from (effectively) localized to (effectively) delocalized: neither limiting case is observed at nonzero subsolidus temperatures. For minerals, such temperatures comprise most terrestrial surface and near-surface occurrences and relevant solid-state experimental protocols. Non-interacting electrons in a periodic lattice potential are not described by free electron (Fermi gas) theory: they are delocalized on a scale comparable to the interatomic distance. Several theoretical constructs are useful in understanding electronic behavior in crystalline systems, beyond the free-electron model: these include Bloch theory (solutions to the Schrödinger equation in a periodic potential, comprising plane waves modulated by the periodicity of the potential), Wannier functions (exponentially-localized orthogonal molecular-orbital wavefunctions for crystalline systems), the tight-binding approximation (approximate Schrödinger-equation solutions based upon linear combinations of atomic orbitals at lattice positions), the Fermi liquid description (the theory, due to Landau, that the ground state of a free-electron gas transforms into the ground state of an interacting system if

the interactions are 'switched on adiabatically', i.e., sufficiently slowly; and the Hubbard model. An excellent introduction to these and related subjects, and many foundational references, are given by Ashcroft and Mermin (1976).

Electronic behavior beyond the Fermi liquid description is said to be *strongly correlated*. In strongly correlated systems, electronic interactions are such that qualitatively new phenomena may emerge [the relevant literature base is monumental; Quintanilla and Hooley (2009) offer a brief, casual overview]. This is the case, for example, when the phase behavior of the system includes a metal-insulator transition, as for vonsenite. The Hubbard model is the theoretical foundation for understanding the behavior of such systems [published work on the Hubbard model begins with Hubbard (1963), and is very extensive]. The model addresses the ability of electrons to 'hop' between atomic sites arranged in crystalline order; this tendency, a function of the electronic kinetic energy, is described by the parameter t (the transfer integral, or hopping integral). Two electrons on the same site incur an interaction energy penalty, U (the Hubbard energy), due to mutual repulsion (the Coulomb interaction is ignored in the Hubbard model; the repulsion arises from the Pauli exclusion principle). The relative magnitudes of the energy terms t and U determine the nature of the correlations between electrons. When $U/t \ll 1$, electrons are almost entirely free to hop, and the material behaves like a metal. When $U/t \gg 1$, electrons are effectively localized at atomic sites, and the material behaves like a magnetic insulator. In intermediate cases, where U/t is 'not too large' in some appropriate sense, superexchange interactions may be possible, and interesting correlations may be observed. This is the case for vonsenite at temperatures of interest in the present study.

Optical opacity and strong pleochroism, observed in vonsenite, are associated with homonuclear and/or heteronuclear intervalence charge transfer (Amthauer and Rossman 1984;

Burns 1991) and with charge delocalization in a low-symmetry environment (Larrea et al. 2001a; Larrea et al. 2001b). These observations suggest at least an intermediate value for U/t.

Triads of the first type (Fe4-Fe2-Fe4) are formed of Fe^{2+}, Fe^{3+} cations in the high-spin d^6 (S = 2), d^5 (S = 5/2) electronic configurations, plus one additional 'itinerant' electron per triad. An average valence of $Fe^{2.53+}$ was determined from structure-refinement data, closely similar to $Fe^{2.5+}$ suggested by Swinnea and Steinfink (1983). Triads of the second type (Fe3-Fe1-Fe3) nominally comprise three Fe^{2+} cations in the high-spin d^6 electronic configurations. We report minor Fe^{3+} also to be present in these sites, as noted above, resulting in an average valence of $Fe^{2.06+}$ as determined from structure-refinement data.

Each triad may be regarded as a rung in a ladder-like structure along [001]; structures of this type are termed three-leg spin ladders (3LLs; Mir et al. 2001). Vonsenite includes two 3LLs: 3LL1 (Fe4-Fe2-Fe4; purple in Fig. 1) and 3LL2 (Fe3-Fe1-Fe3; blue in Fig. 1). Electronic interactions are observed within 3LL1 rungs due to short Fe2-Fe4 distances (2.783 Å at 295 K; Table 3). Much greater distances between Fe1 and Fe1, Fe2 and Fe2, Fe3 and Fe3, and Fe4 and Fe4 (all ~ 3.07 Å); Fe1 and Fe3 (~ 3.09 Å), Fe1 and Fe4 (~ 3.10 Å), Fe2 and Fe3 (~ 3.17 Å), Fe3 and Fe4 (~ 3.19 Å), and Fe1 and Fe2 (~3.38 Å) cause interactions between 3LL1 and 3LL2, and 3LL2 intra-rung interactions, to be "very weak" (Bordet and Suard 2009). This conclusion is at variance with that of Swinnea and Steinfink (1983) ("At room temperature a mechanism of charge delocalization over the complete structure is also operative"), and the claim of Burns (1993) in support of "structure-wide intervalence charge transfer" in vonsenite.

Peierls (1930) established that an external sinusoidal potential of wavenumber q opens an energy gap at $k = \pm q/2$ in the band structure of a one-dimensional free-electron gas. For $q = 2k_F$, where k_F is the Fermi wavenumber (the radius in k-space of the Fermi surface for the one-

dimensional free-electron gas), an energy gap of magnitude 2□, from E_F + □ to E_F - □, where E_F is the Fermi energy, is opened at $k = \pm k_F$. Note that Peierls's assumption of a free-electron gas is incompatible with the Hubbard model.

Frölich (1954) and Peierls (1955) expanded upon Peierls (1930), establishing that a periodic chain with one electron per atom (i.e., a half-filled one-dimensional energy band) is unstable to a periodic lattice distortion (PLD). The Peierls instability induces a structural phase transition in which every other cation in a one-dimensional chain moves nearer to one neighbor and further away from the other. This periodic lattice distortion is referred to as dimerization or, more generally, a charge density wave [see Thorne (1996) for an informal overview of charge density waves; Di Salvo and Rice (1979) for a presentation at similar level with emphasis on incommensurate structures in transition-metal compounds; and the formal review of Grüner (1988)]. The PLD phenomenon was first observed by Comès et al. (1973), in the one-dimensional conductor (i.e., '1-D metal') $K_2Pt(CN)_4Br_{0.30}{\cdot}xH_2O$.

Dimerization results in the appearance of a band gap in the electronic energy spectrum at precisely the Fermi momentum, $p_F = \hbar k_F$, the momentum of an electron at the Fermi surface. As a result, the energies of electronic states at or below (within) the Fermi surface are reduced, and the energies of electronic states above (outside) the Fermi surface are increased. At sufficiently low temperatures (including temperatures of interest in the present work), essentially all those states with lowered energies are occupied and all those with raised energies are unoccupied, with the result that the total energy of the charge-density-wave state is lower than that of the initial, undistorted state. So it is that a 1-D metal is inherently unstable to a charge-density wave, the result known as the Peierls theorem.

Systems exhibiting the Peierls instability are called Peierls systems; the 3LL1 ladder in synthetic endmember vonsenite, with a single itinerant electron per triad rung, is proposed by Bordet and Suard (2009) to be a Peierls system. More precisely, it is a 1-D Peierls-like system (Latgé and Continentino 2002).

The work of Peierls and Fröhlich was largely ignored or forgotten (Pouget 2016) until the late 1970s, when PLDs and the metal-insulator phase transition became topics of considerable research interest, specifically in context of 1-D metals. McConnell (1983) applied the nascent theory of charge-density waves in insulators to modulated or incommensurate mineral structures, integrating the Landau theory of continuous phase transitions with *k*-space symmetry concepts, group theory, and band theory. Peierls (1955) is cited, but the Peierls theorem is not mentioned, and no Peierls- or Peierls-like instability is illustrated or discussed. Like Peierls, McConnell (1983) omits any discussion of electronic interactions.

McConnell (1983) gives a justification for this approach: "The advantage of approaching the problem of the origin of incommensurate mineral structures from this point of view is that the general theory can then be tested by direct reference to symmetry and structural data for a number of mineral systems." It is perhaps for this reason that, so far as the present authors are aware, Peierls transitions have not been reported as such in a mineralogical context, despite a very extensive body of published work on modulated mineral structures. For fuller discussions of the Peierls instability, Peierls-like instabilities, and charge density waves in relevant context, see, e.g., Latgé and Continentino (2002) and especially the authoritative review of Pouget (2016) and references therein. The very recent work of Kartoon et al. (2019) proposes that electronic interactions and the electronic kinetic energy (not considered by Peierls or Frölich; introduced by Hubbard, a decade later) are likely to underlie the Peierls instability.

As temperature is reduced below approximately 283 K, the 3LL1 triad rungs in synthetic endmember vonsenite exhibit a charge-ordering transition arising from a Peierls-like instability. Charge ordering (CO), the long-range ordering of transition-metal oxidation states (Attfield 2006), may be observed in phases exhibiting strong electronic correlations. In the simplest manifestation of charge ordering, above a transition temperature, T_{CO}, a polyvalent cation in an average (i.e., non-integral) oxidation state occupies a specific crystallographic site, or symmetry-equivalent sites, in a material of a given space-group symmetry; cation valences at these sites may be estimated by the bond valence sum method. Below T_{CO}, the phase undergoes a symmetry-breaking transition, a continuous or second-order phase transition to a structural state of reduced (i.e., broken) symmetry; the space-group symmetry of the broken-symmetry phase must be a subgroup of the symmetry group of the higher-symmetry phase prior to the phase transition (see, e.g., Low and Manohar 2002).

CO may be site-centered, wherein the relevant crystallographic sites after the ordering transition are inequivalent to those before the transition, as observed in the heterovalent-iron inverse spinel magnetite, $Fe^{3+}[Fe^{2.5+}]_2O_4$ (Verwey 1939; Wright et al. 2001, 2002; Senn et al. 2012) and in perovskite manganites (Mostovoy 2006; Yamada et al. 2014). Quasi-one-dimensional Peierls systems exhibit bond-centered charge ordering, wherein the sites remain equivalent after the transition but the bonds do not. Efremov et al. (2005) present calculations supporting the coexistence of site-centered- and bond-centered charge ordering in perovskite manganites. Charge ordering in vonsenite, a Peierls-like system (Latgé and Continentino 2002), with stronger intra-dimer bonds alternating with weaker bonds between dimers, and also site-splitting, resulting in symmetrically inequivalent sites in the low-temperature, broken-symmetry,

post-transition phase, appears to manifest the bond-centered/site-centered duality predicted by Efremov et al. (2005) for perovskite manganites.

The spin ladder 3LL1 is the locus of the Peierls-like instability that induces the 283 K phase transition observed in synthetic vonsenites. Below the charge-ordering temperature, $T_{CO} \sim$ 283 K, the single itinerant electron per Fe4-Fe2-Fe4 triad rung of 3LL1 dimerizes the Fe-cation sites alternately, perpendicular to [001] (whence *transverse* charge density wave: see Fig. 2), associating Fe4 with the Fe2 to its right (the dimerized Fe4 is relabelled as Fe4a; the undimerized Fe4 to the left of Fe2 becomes Fe4b); in the adjacent rung, Fe2 dimerizes with the Fe4 site to its right, then Fe4 with Fe2, and so on along [001], doubling the *c*-axis period and creating an *n*-glide along [010]. Period-doubling creates a band gap in the electronic density of states, at $\pm k_F$, causing a transition from metallic to insulating behavior: a metal-insulator transition. Thus the 283 K *Pbam*/*Pbnm* structural transition observed in synthetic endmember vonsenite is at once a charge ordering transition, a symmetry-breaking transition, and a metal-insulator transition.

The described structural rearrangement reported in synthetic specimens is observed as well in the present study of a natural vonsenite, on the basis of structure refinements with significantly improved *R*-values compared to those reported in previous structure studies. Space group *Pbnm* is confirmed at temperatures below 283 K for which structure data were obtained: 100K (R_1 = 0.0186), and 90 K (R_1 = 0.0183). One crystallographic consequence of the phase transition is the bifurcation of the Fe4 *Pbam* site to the non-equivalent Fe4a and Fe4b sites in *Pbnm*, illustrated schematically in Figure 2, as reported first by Mir et al. (2001) in a synthetic vonsenite. The Mir et al. (2001) data at 294 K and 144 K are closely similar to those presented here at 295 K and 100 K: we report Fe4 – Fe2 = 2.783 Å at 295 K to their 2.786 Å at 294 K; Fe4a – Fe2 = 2.621 Å at 100 K to their 2.616 Å at 144 K; and Fe4b – Fe2 = 2.931 Å to their

2.942 Å at those same temperatures. We acknowledge also the observation of Bordet and Suard (2009) (who collected data at 290 K, 300 K, and 320K, as well as at lower temperatures to investigate magnetic transitions), who "could detect superstructure spots characteristic of a doubling of the *c* axis parameter already on the 290K data", suggesting that the phase transition, reported by Mir et al. (2001) as "reversible" and occurring at 283 K, may be of second order, i.e., continuous, with a nonzero value for the order parameter above the notional critical temperature $T_c \sim 283$ K.

Vonsenite exhibits an antiferromagnetic phase transition at 114 K, and a ferromagnetic phase transition at 70 K (noted above in the discussion of Mössbauer results), which are interpreted as indicating the presence of two independent magnetic subsystems (Bordet and Suard 2009) with orthogonal magnetic orderings (Knyazev et al. 2019). The triangular arrangement of Fe cations between 3LL1 and 3LL2 (Figure 2) suggests that significant geometrical frustration of superexchange interactions would be observed. The orthogonal orientations of the magnetic ordering in 3LL1 and 3LL2 effectively decouples these two subsystems, with the result that the anticipated frustration is almost entirely quenched. (Knyazev et al. 2019) present a detailed analysis of these interactions.

IMPLICATIONS

Vonsenite, a relatively poorly known mineral, has been of considerable interest in the condensed-matter-physics and materials-science communities since the work of Swinnea and Steinfink (1983). The entirety of that interest has been focused upon synthetic vonsenite of ideal endmember composition, a phase that exhibits subtle and complex electronic, magnetic and ordering behavior, multiferroicity, and a *Pbam*/*Pbnm* phase transition at or below approximately

283 K. By contrast, the structure and properties of natural vonsenites – as opposed to their occurrence and paragenesis – have been accorded essentially no attention by the mineralogical community.

Peierls- and Peierls-like instabilities or distortions, and the charge-ordering-, symmetry-breaking, and/or metal-insulator transitions arising from such instabilities, are not uncommon in heterovalent materials under terrestrial conditions in laboratory settings. The mechanism of the Verwey metal-insulator transition at T_{Verwey} ~122 K in the ferrimagnetic inverse spinel magnetite, which continues to defy consensus explication despite 80 years of study, is the perhaps the best-known and most extensively studied mineralogical example. Shchennikov and Ovsyannikov (2009) present a Peierls model that is consistent with published structural and spectroscopic data for magnetite, and propose that a Peierls instability may underlie the Verwey transition, with $T_{Peierls} \sim T_{Verwey}$. Identification of a Peierls instability in such a familiar mineral would suggest the possibility that the Peierls instability may underlie structural phase transitions in other minerals as well, potentially offering deeper insights into phenomena that are understood incompletely or incorrectly at present.

Bozin et al. (2019) describe a *d*-orbital-degeneracy-lifted phenomenon revealed by "difficult to detect but important local structural variations" – possibly analogous to the small splittings detected for Fe2, B, O1, O3, and O5 in the present work and noted above – as evidence of a Peierls-instability-related, local, fluctuating, orbital-degeneracy-lifted high-temperature state "likely to be widespread amongst diverse classes of partially filled nominally degenerate *d*-electron systems". We encourage investigators to be open to the possibility of similar phenomena in mineral phases for which *d*-electron interactions are relevant.

ACKNOWLEDGMENTS

Support for this work was provided by the National Science Foundation through grant NSF-MRI 1039436 to JMH. Edward Bonner worked on early structure refinements of vonsenite. MM expresses deep gratitude for the privilege of having been a student of Charles T. Prewitt and the late Roger G. Burns. Consummate experimentalists, visionary thinkers, mentors at once thoughtful and demanding, Charlie and Roger are lions of mineralogy, central to the evolution and transformation of the discipline from its descriptive origins to a quantitative science with a nascent capacity for prediction: from *what*, to *how* and *why*. The manuscript was improved by reviews by two anonymous reviewers and a Technical Reviewer, and expertly handled by Associate Editor Aaron Lussier, for which we are very appreciative; thanks are also due to the *American Mineralogist* Technical Editor team for discussion of detection of the superstructure in an early manuscript version.

REFERENCES CITED

Amthauer, G., and Rossman, G. R. (1984) Mixed Valence of Iron in Minerals with Cation Clusters. Physics and Chemistry of Minerals, 11, 37-51.

Ashcroft, N. W. and Mermin, N. D. (1976) Solid State Physics. Holt, Rinehart and Winston.

Attfield, J. P. (2006) Charge ordering in transition metal oxides. Solid State Sciences, 8, 861-867.

Biryukov, Y. P., Zinnatullin, A. L., Bubnova, R. S., Vagizov, F. G., Shablinskii, A. P., Filatov, S. K., Shilovskikh, V. V., and Pekov, I. V. (2020) Investigation of thermal behavior of mixed-valent iron borates vonsenite and hulsite containing $[OM_4]^{n+}$ and $[OM_5]^{n+}$ oxocentred polyhedra by in situ high-temperature Mössbauer spectroscopy, X-ray diffraction and thermal analysis. Acta Crystallographica, B76, 543-553.

Bonazzi, P., and Menchetti, S. (1989) Contribution to the crystal chemistry of the minerals of the ludwigite-vonsenite series. Neues Jahrbuch für Mineralogie, Monatshefte, 1989, 69-83.

Bozin, E.S., Yin, W.G., Koch, R.J., Abeykoon, M., Hor, Y.S., Zheng, H., Lei, H.C., Petrovic, C., Mitchell, J.F., and Billinge, S.J.L. (2019) Local orbital degeneracy lifting as a precursor to an orbital-selective Peierls transition. Nature Communications, 10, 3638-3644.

Bordet, P., and Suard, E. (2009) Magnetic structure and charge ordering in Fe_3BO_5: A single-crystal x-ray and neutron powder diffraction study. Physical Review B, 79, 144408-144408-7.

Burns, R. G. (1981) Intervalence transitions in mixed-valence minerals of iron and titanium. Annual Reviews of Earth and Planetary Sciences, 9, 345-383.

Burns, R. G. (1991) Mixed Valency Minerals: Influences of Crystal Structures on Optical and Mössbauer Spectra, in Mixed Valency Systems: Applications in Chemistry, Physics and

Biology. K. Prassides, Ed. NATO ASI Series Volume 343 (Series C: Mathematical and Physical Sciences). Springer, Dordrecht. 175-199.

Burns, R. G. (1993) Mineralogical Applications of Crystal Field Theory, Second Edition. Cambridge University Press.

Cherkezova-Zheleva, Z., Tsoncheva, T., Tyuliev, G., and Mitov, I. (2006) Study of mixed valence iron borate catalysts in ethyl acetate oxidation process. Applied Catalysis A, 298, 24-31.

Comès, R., Lambert, M., Launois, H., and Zeller, H. R. (1973) Evidence for a Peierls Distortion or a Kohn Anomaly in One-Dimensional Conductors of the Type $K_2Pt(CN)_4Br_{0.30}{\cdot}xH_2O$. Physical Review B, 8, 571-575.

de Grave, E., and van Alboom, A. (1991) Evaluation of ferrous and ferric Mössbauer fractions. Physics and Chemistry of Minerals, 18, 337–342.

Di Salvo, F. J., Jr., and Rice, T. M. (1979) Charge-density waves in transition-metal compounds. Physics Today, 32, 32-38.

Douvalis, A.P., Moukarika, A., Bakas, T., Kallias, G., and Papefthymiou, V. (2002) Mössbauer and magnetization studies of Fe_3BO_5. Journal of Physics: Condensed Matter, 14, 3303-3320.

Douvalis, A.P., Papaefthymiou, V., Bakas, T., and Moukarika, A. (1997) Magnetic hysteresis in novel magnetic materials (NATO ASI Series vol. 338), G.C. Hadjipanayis, Ed. Dordrecht, Kluwer. 761-765.

Efremov, D. V., van den Brink, J., and Khomskii, D. M. (2005) Bond centered vs. site-centered charge ordering: ferroelectricity in oxides. Physica B, 359-361, 1433-1435.

Frölich, H. (1954) On the theory of superconductivity: the one-dimensional case. Proceedings of the Royal Society of London, Series A, Mathematical and Physical Sciences, 223, 296-305.

Grüner, G. (1988) The dynamics of charge-density waves. Reviews of Modern Physics, 60, 1129-1181.

Guimarães, R.B., Mir, M., Fernandes, J.C., Continentino, M.A., Borges, H.A., Cernicchiaro, G., Fontes, M.B., Candela, D.R.S., and Baggio-Saitovich, E. (1999) Cation-mediated interaction and weak ferromagnetism in $Fe_3O_2BO_3$. Physical Review B, 60, 6617-6622.

Hubbard, J. (1963) Electron Correlations in Narrow Energy Bands. Proceedings of the Royal Society of London, Series A, Mathematical and Physical Sciences, 276, 238-257.

Kartoon, D., Argaman, U., and Makov, G. (2019) The driving force behind the distortion of one-dimensional monatomic chains – Peierls theorem revisited. arXiv:1906.03421v1.

Knyazev, Y. V., Kazak, N. V., Nazarenko, I. I., Sofronova, S. N., Rostovtsev, N. D., Bartolome, J., Arauzo, A., and Ovchinnikov, S. G. (2019) Effect of magnetic frustrations on magnetism of the Fe_3BO_5 and Co_3BO_5 ludwigites. Journal of Magnetism and Magnetic Materials, 474, 493-500.

Larrea, A., Sanchez, D. R., Baggio-Saitovitch, E. M., Fernandes, J. C., Guimarães, R. B., Continentino, M. A., and Litterst, F. J. (2001a) Magnetism and charge ordering in $Fe_3O_2BO_3$ ludwigite. Journal of Magnetism and Magnetic Materials, 226-230, 1079-1080.

Larrea, A., Sanchez, D. R., Litterst, F. J., and Baggio-Saitovitch, E. M. (2001b) Charge delocalization in ludwigite $Fe_3O_2BO_3$. Journal of Physics: Condensed Matter, 13, L949-L954.

519 Latgé, A., and Continentino, M. A. (2002) Transverse charge density waves in ladder systems.
520 Physical Review B, 66, 094113-1 – 094113-5.
521 Li, Z., Stevens, J.G., and Zhang, Y. (1994) Mixed valence of iron in natural vonsenite. Hyperfine
522 Interactions, 83, 489-494.
523 Low, I., and Manohar, A. V. (2002) Spontaneously Broken Spacetime Symmetries and
524 Goldstone's Theorem. Physical Review Letters, 88, 101602-1 – 101602-4.
525 Maignan, A., Lainé, F., Guesdon, A., Maol, S., Damay, F., and Martin, C. (2017) Charge
526 ordering and multiferroicity in Fe_3BO_5 and Fe_2MnBO_5 oxyborates. Journal of Solid State
527 Chemistry, 246, 209-213.
528 McConnell, J. D. C. (1983) A review of structural resonance and the nature of long-range
529 interactions in modulated mineral structures. American Mineralogist, 68, 1-10.
530 Mir, M., Guimarães, R.B., Fernandes, J.C., and Continentino, M.A., Doriguetto, A. C.,
531 Mascarenhas, J. Ellena, and Castellano, E. E.; Freitas, R. S., and Ghivelder, L. (2001)
532 Structural Transition and Pair Formation in $Fe_3O_2BO_3$. Physical Review Letters, 87,
533 1472012-1 – 1472012-4.
534 Mitov, I., Cherkezova-Zheleva, Z., Mitrov, B., and Kunev, B. (1999) Mechanochemical
535 synthesis of ferroferriborate (vonsenite, Fe_3BO_5) and magnesium ferroferriborate
536 (ludwigite, Fe_2MgBO_5). Journal of Alloys and Compounds, 289, 55-65.
537 Mokeyeva, V.L. (1968) Refinement of structure of ludwigite ($Mg_{1.85}$ $Fe_{0.15}^{2+}$)($Fe_{0.60}^{3+}$
538 $Al_{0.40}$)BO_3O_2 and distribution of Mg^{2+} and Fe^{2+} among the cation sites of the structure.
539 Geochemistry International, 5, 809–13.
540 Mostovoy, M. (2006) Ferroelectricity in Spiral Magnets. Physical Review Letters, 96, 067601-1–
541 067601-4.

Palache, C., Berman, H., and Frondel, C. (1951) The System of Mineralogy of James Dwight Dana and Edward Salisbury Dana, Yale University 1837-1892, Volume II: Halides, Nitrates, Borates, Carbonates, Sulfates, Phosphates, Arsenates, Tungstates, Molybdates etc., 7th edition, revised and enlarged. 321-324. John Wiley and Sons, Inc., New York.

Peierls, R. E. (1930) Zur Theorie der elektrischen und thermischen Leitfähigkeit von Metallen. Annalen der Physik Leipzig, 4, 121-148.

Peierls, R. E. (1955) Quantum Theory of Solids. Clarendon Press, Oxford.

Pouget, J.-P. (2016) The Peierls instability and charge density wave in one-dimensional electronic conductors. Comptes Rendus Physique, 17, 332-356.

Quintanilla, J. and Hooley, C. (2009) The strong-correlations puzzle. Physics World, June 2009, 32-37.

Senn, M. S., Wright, J. P., and Attfield, J. P. (2012) Charge order and three-site distortions in the Verwey structure of magnetite. Nature, 481, 173-176.

Shchennikov, V.V., and Ovsyannikov, S.V. (2009) Is the Verwey transition in Fe_3O_4 magnetite driven by a Peierls distortion? Journal of Physics: Condensed Matter, 21, 1-4.

Sheldrick, G. M. (2008) A short history of SHELX. Acta Crystallographica A, 64, 112-122.

Sofronova, S., and Nazarenko, I. (2017) Ludwigite: From natural mineral to modern solid solutions. Crystal Research and Technology, 52, 1600338-1-1600338-19.

Swinnea, J. S., and Steinfink, H. (1983) Crystal structure and Mössbauer spectrum of vonsenite, $2FeO{\cdot}FeBO_3$. American Mineralogist, 68, 827-832.

Takéuchi, Y. (1956) The Crystal Structure of Vonsenite. Mineralogical Journal, 2, 19-26.

Takéuchi, Y., Watanabé, T., and Ito, T. (1950) The crystal structures of warwickite, and pinakiolite. Acta Crystallographica, 3, 98-107.

565 Thorne, R. E. (1996) Charge-Density-Wave Conductors. Physics Today, 49, 42-47.

566 Tschermak, G. (1874) Ludwigit, ein neues Mineral aus dem Banate. Mineralogische und
567 petrographische Mitteilungen, gesammelt von Gustav Tschermak. Wilhelm Braumüller,
568 Vienna. 59-66.

569 van den Brink, J., and Khomskii, D. I. (2008) Multiferroicity due to charge ordering. Journal of
570 Physics: Condensed Matter, 20, 434217-434229.

571 Verwey, E. J. W. (1939) Electronic Conduction of Magnetite (Fe_3O_4) and its Transition Point at
572 Low Temperatures. Nature, 144, 327.

573 Wills, A.S. (2020) *VaList*, Program available from www.ccp14.ac.uk.

574 Wright, J. P., Attfield, J. P., and Radaelli, P. G. (2001) Long Range Charge Ordering in
575 Magnetite Below the Verwey Transition. Physical Review Letters, 87, 266401-1 -
576 266401-4.

577 Wright, J. P., Attfield, J. P., and Radaelli, P. G. (2002) Charge ordered structure of magnetite
578 below the Verwey transition. Physical Review B, 41, 214422-1 - 214422-15.

579 Xuemin, K., Hongsen, X., Yirong, L., and Enlin, Z. (1984) The magnetically-ordering of
580 ludwigite and synthetic vonsenite and their Mössbauer spectra. Kexue tongbao, 29, 928-
581 931.

582 Yamada, I., Etani, H., Murakami, M., Hayashi, N., Kawakami, T., Mizumake, M., Ueda, S., Abe,
583 H., Liss, K.-D., Studer, A. J., Osaka, T., More, S., Takahashi, R, and Irifune, T. (2014)
584 Charge-Order Melting in Charge-Disproportionated Perovskite $CeCu_3Fe_4O_{12}$. Inorganic
585 Chemistry, 53, 11794-11801.

586

587
588

589

This is the peer-reviewed, final accepted version for American Mineralogist, published by the Mineralogical Society of America.
The published version is subject to change. Cite as Authors (Year) Title. American Mineralogist, in press.
DOI: https://doi.org/10.2138/am-2021-7851. http://www.minsocam.org/

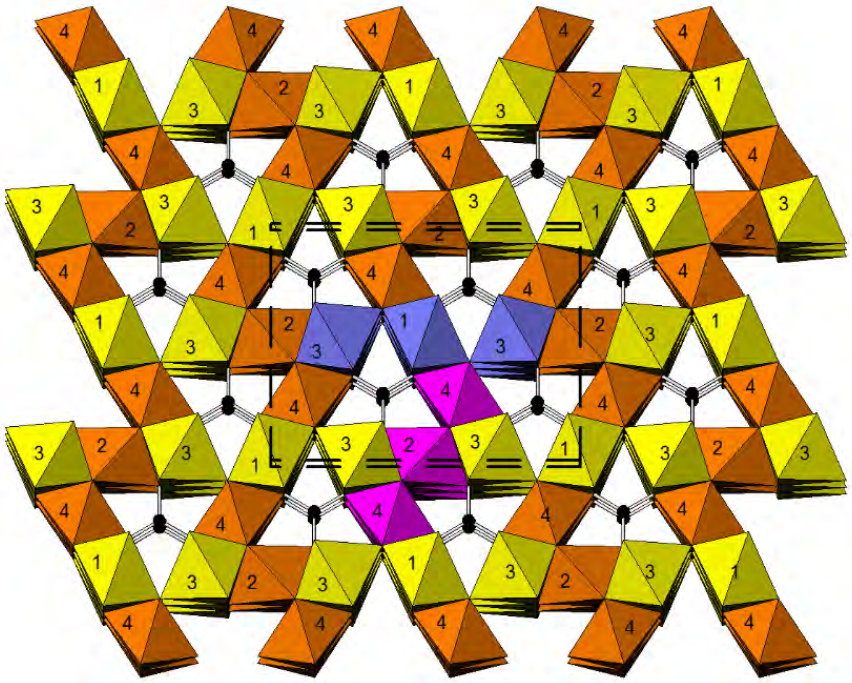

FIGURE 1. Atomic arrangement of vonsenite at 295° rotated 5 degrees around *b* from a (001) projection. Individual FeO_6 octahedra are labeled (1 = Fe1, etc.). A single Fe4-Fe2-Fe4 Type 1 triad is shown in purple; a single Fe3-Fe1-Fe3 Type 2 triad is shown in blue.

This is the peer-reviewed, final accepted version for American Mineralogist, published by the Mineralogical Society of America.
The published version is subject to change. Cite as Authors (Year) Title. American Mineralogist, in press.
DOI: https://doi.org/10.2138/am-2021-7851. http://www.minsocam.org/

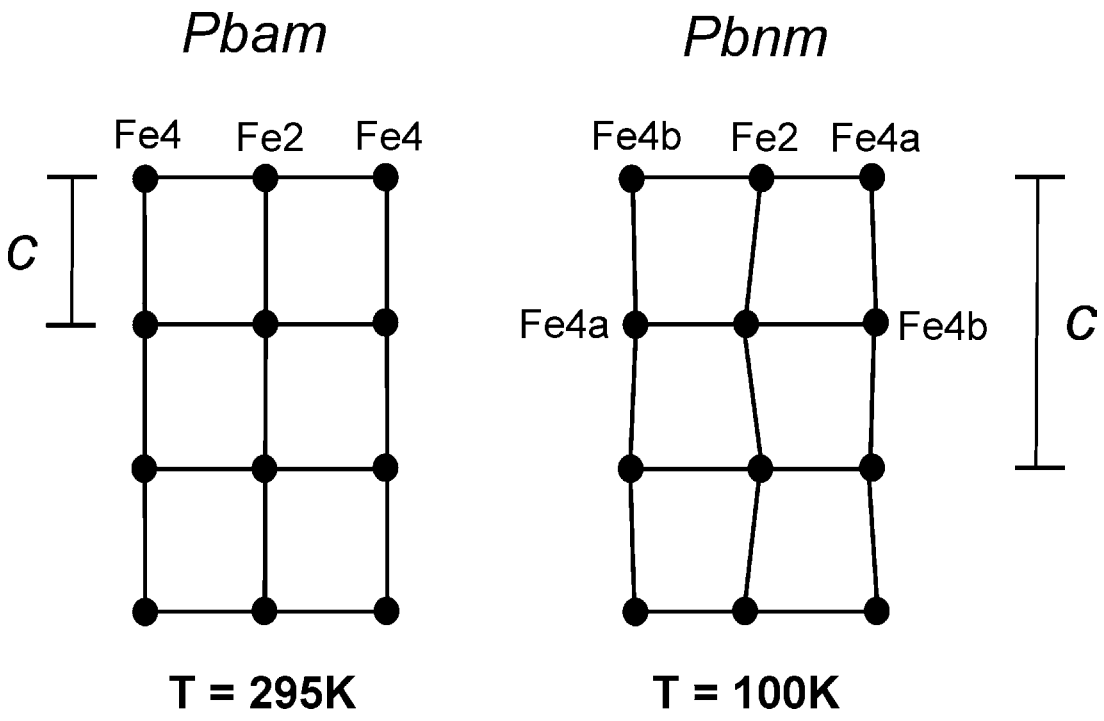

FIGURE 2. Fe4-Fe2-Fe4 3LL1 three-leg ladder in vonsenite, above (*Pbam*) and below (*Pbnm*) the ~ 283 K structural transition temperature, as reported in synthetic vonsenite and observed in the natural specimen of the present study. Adapted from Bordet and Suard (2009).

618

This is the peer-reviewed, final accepted version for American Mineralogist, published by the Mineralogical Society of America.
The published version is subject to change. Cite as Authors (Year) Title. American Mineralogist, in press.
DOI: https://doi.org/10.2138/am-2021-7851. http://www.minsocam.org/

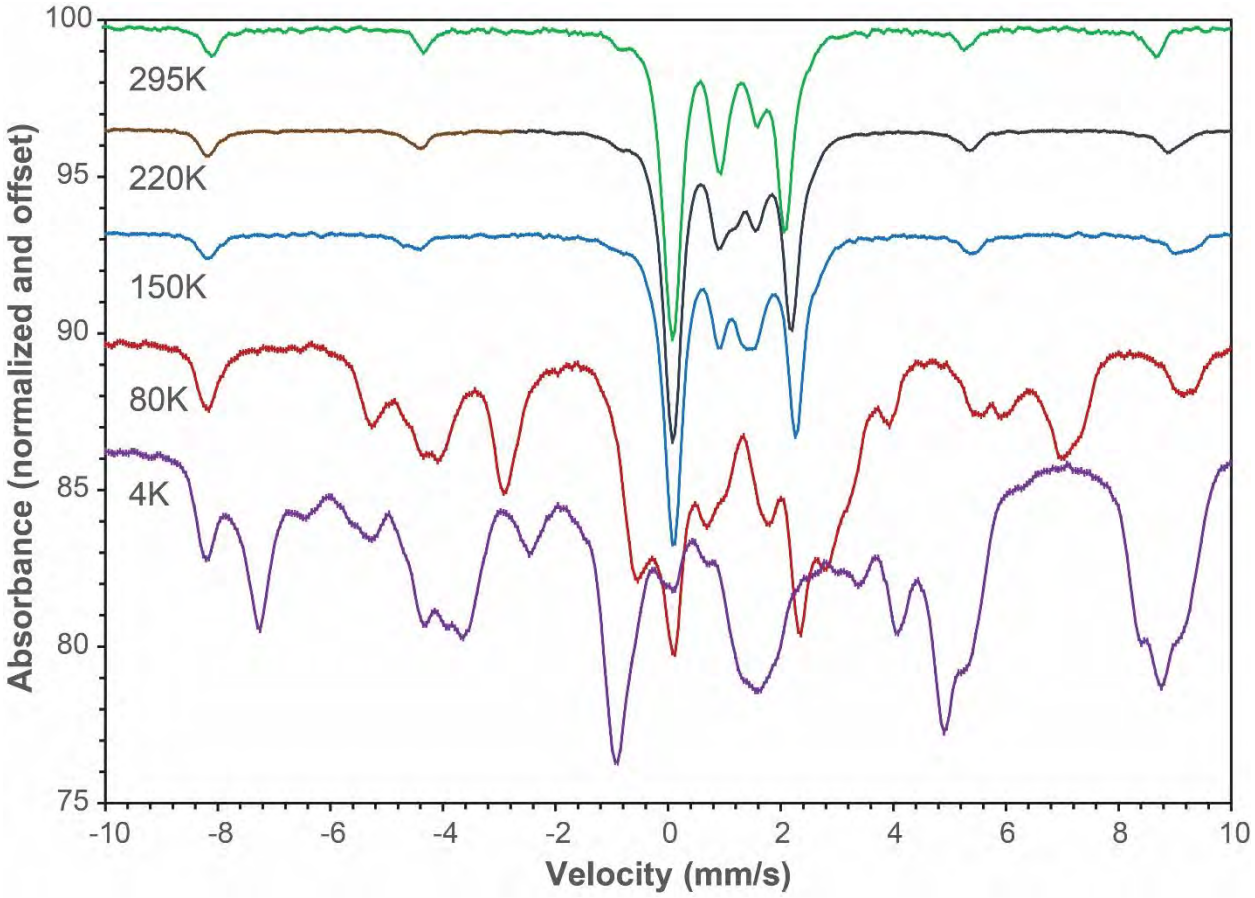

FIGURE 3. Stacked Mössbauer spectra showing relationships among data acquired at 295, 220, 150, 80, and 4 K.

This is the peer-reviewed, final accepted version for American Mineralogist, published by the Mineralogical Society of America.
The published version is subject to change. Cite as Authors (Year) Title. American Mineralogist, in press.
DOI: https://doi.org/10.2138/am-2021-7851. http://www.minsocam.org/

631

632

633

634

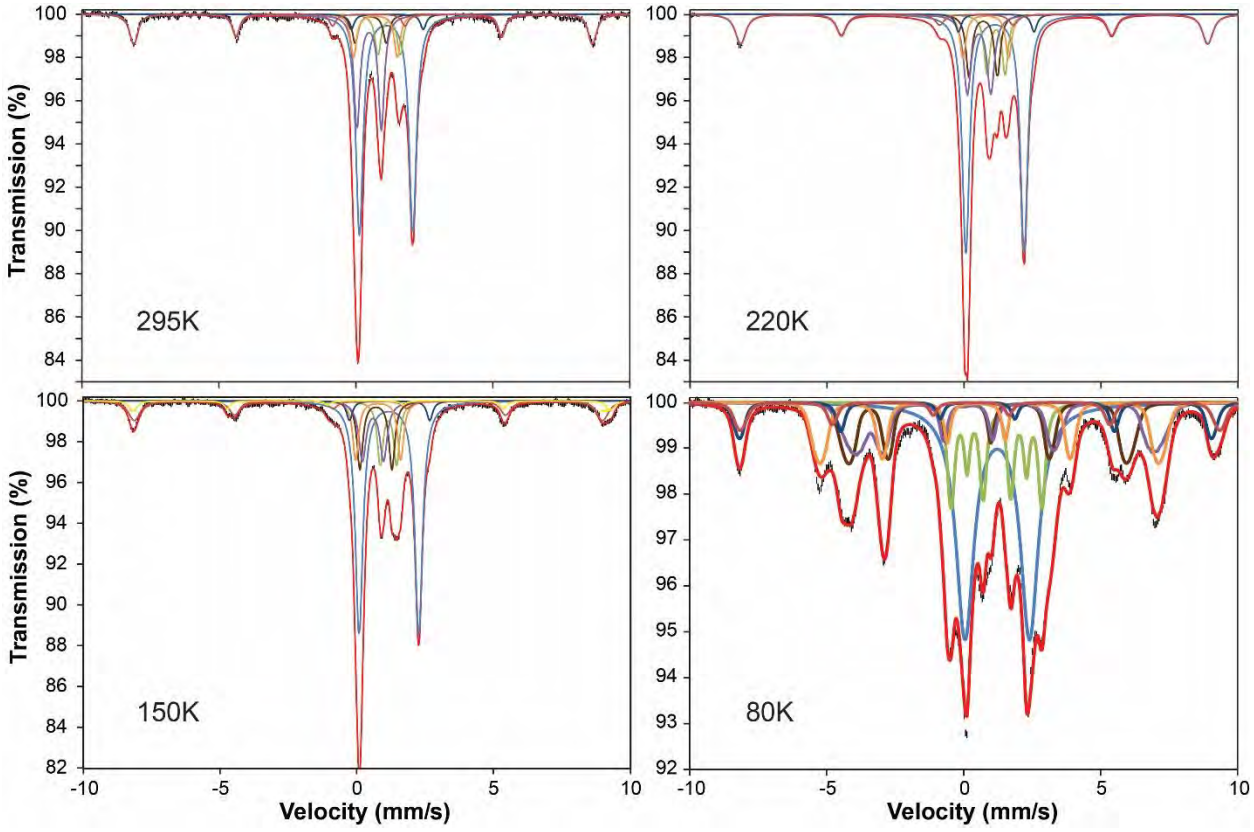

635

636

637 **FIGURE 4**. Fits to Mössbauer spectra acquired at 295, 220, 150, and 80 K.

638

639

This is the peer-reviewed, final accepted version for American Mineralogist, published by the Mineralogical Society of America.
The published version is subject to change. Cite as Authors (Year) Title. American Mineralogist, in press.
DOI: https://doi.org/10.2138/am-2021-7851. http://www.minsocam.org/

TABLE 2. Fe^{2+}/Fe^{3+} site occupancy (%) for Fe sites in vonsenite based on SREF (calculated using VaList; Wills, 2020).

	295K		100K		90K	
Atom	Fe^{2+}	Fe^{3+}	Fe^{2+}	Fe^{3+}	Fe^{2+}	Fe^{3+}
Fe1	96	4	95	5	94	6
Fe2	64	36	60	40	60	40
Fe2'	--	--	49	51	48	52
Fe3	93	7	92	8	92	8
Fe4	38	62	--	--	--	--
Fe4a			49	51	49	51
Fe4b			26	74	21	79

Cell parameters:
295: $a = 9.4446(6)$, $b = 12.3019(8)$, $c = 3.0743(2)$
100: $a = 9.4322(14)$, $b = 12.2819(19)$, $c = 6.1486(9)$
90: $a = 9.4318(15)$, $b = 12.283(2)$, $c = 6.1492(10)$

This is the peer-reviewed, final accepted version for American Mineralogist, published by the Mineralogical Society of America.
The published version is subject to change. Cite as Authors (Year) Title. American Mineralogist, in press.
DOI: https://doi.org/10.2138/am-2021-7851. http://www.minsocam.org/

676

677

678 **TABLE 3**. Fe-Fe distances (< 3.1Å) in vonsenite (Å). Distances <3.0Å in bold.

679

	295 K		**100 K**	**90 K**
Fe1-Fe1	3.074	**Fe1**-Fe1	3.074	3.075
-Fe4	3.098	-Fe4b	3.082	3.082
Fe2-Fe4	**2.783**	**Fe2-**Fe4a	**2.621**	**2.622**
-Fe2	3.074	-Fe4b	**2.931**	**2.930**
		-Fe2	3.083	3.083
Fe3-Fe3	3.074			
		Fe2'- Fe4b	**2.664**	**2.658**
Fe4-Fe2	**2.783**	-Fe4a	**2.888**	**2.894**
-Fe4	3.074	-Fe2	3.075	3.075
-Fe1	3.098	-Fe2'	3.090	3.092
		Fe3-Fe3	3.051	3.051
		-Fe3	3.098	3.099
		Fe4a-Fe2	**2.621**	**2.622**
		-Fe2'	**2.888**	**2.894**
		-Fe4b	3.075	3.076
		Fe4b-Fe2'	**2.664**	**2.658**
		-Fe2	**2.931**	**2.930**
		-Fe4a	3.075	3.076
		-Fe1	3.082	3.082

680

681

682

683

684

SUBSEQUENT TABLES FOR DEPOSIT

691

692

693

694 **TABLE 1**. Electron microprobe analysis of natural vonsenite.

695

Fe	61.16(70)
Al	0.23(2)
Mn	0.33(4)
V	0.01(3)
Ti	0.05(1)
Mg	0.74(4)
B_{calc*}	4.11
O_{calc*}	30.43
Total	97.06

696

697 *B and O calculated to be stoichiometric. Empirical formula =
698 $(Fe^{2+}_{1.90}\ Mg_{0.08}Mn^{2+}_{0.02})_{\Sigma 2.00}(Fe^{3+}_{0.98}Al_{0.02})_{\Sigma=1.00}BO_5$;
699 formula basis (Fe+Mg+Mn+Al+Ti+V) = 3.
700
701

702

703
704

705

706
707

708

TABLE 4a. Mössbauer parameters for vonsenite.

Parameter	**Douvalis et al. (2002)**				**This study**		**Douvalis et al. (2002)**
Temperature	**Assignment**	**116**	**80**	**150**	**220**	**295**	**270**
CS(mm/s)		1.21	1.23	1.18	1.13	1.11	1.10
QS(mm/s)	D1 Fe1‡ or Fe1/Fe3§	2.22	2.36	2.18	2.13	1.95	2.03
Width(mm/s)		0.14	0.79	0.33	0.32	0.32	0.16
Area (%)*		17	39.3	59.5	58.7	59.0	16
CS(mm/s)		1.21	1.21				1.10
QS(mm/s)		2.19	2.11				2.04
Field(KOe)	D2 Fe4‡ or Fe2/Fe4§	0.14	49				0.16
Omega(degree)			56				33
Width(mm/s)			0.26†				
Area (%)*		33	15.7				
CS(mm/s)		0.51	0.54	0.60	0.55	0.49	0.47
QS(mm/s)		0.82	0.69	0.77	0.86	0.89	0.77
Field(KOe)	D3 Fe2/Fe3‡	0.12	313				0.13
Omega(degree)	or Fe2/Fe4§	17	0.26†	0.33	0.33	0.27	17
Width(mm/s)			13	11	15	20	
Area (%)			14.6	14.9	20.0	25.6	
CS(mm/s)		0.85	0.83	0.79	0.79	0.72	0.77
QS(mm/s)		1.36	1.42	1.65	1.67	1.60	1.48
Field(KOe)	D4 Fe2/Fe3‡	0.12	335				0.14
Omega(degree)	or Fe1/Fe3§	16	10				17
Width(mm/s)			0.30†	0.26†	0.26†	0.26†	
Area (%)*			15.7	12.2	9.3	9.0	
CS(mm/s)		0.80	0.70	0.70	0.70	0.54	0.69
QS(mm/s)	D5 Fe2/Fe3‡ or	1.11	1.21	1.17	1.04	1.14	0.97
Field(KOe)	Fe2/Fe4§	0.12	376				0.14

Omega(degree)	17	38				17
Width(mm/s)		0.26†	0.26†	0.26†	0.26†	
Area (%)		14.6	13.5	12.0	6.4	
Chi-squared		5.2	0.9	2.4	0.8	

709

*Peak areas are normalized to reflect only the % of iron in the vonsenite. Full fit parameters including impurities are given in the supplement. †Linewidth held constant at this value. ‡Assignment based on Douvalis et al. (2002). §Assignment from this paper.

710
711
712

713

This is the peer-reviewed, final accepted version for American Mineralogist, published by the Mineralogical Society of America.
The published version is subject to change. Cite as Authors (Year) Title. American Mineralogist, in press.
DOI: https://doi.org/10.2138/am-2021-7851. http://www.minsocam.org/

714 **TABLE 4b.** Supplementary Mössbauer parameters for vonsenite.

715

716

	4K	4K alt	80K	150K	220K	295K	
	18013101a	18013101d	18013102e	18020101c	18020201	18012905b	
CS(mm/s)				1.21	1.174	1.147	
QS(mm/s)				2.94	2.76	2.626	Olivine-like but could be any octahedral ferrous
Width(mm/s)				0.26*	0.26*	0.26*	
Area (%)				3	3	3	
CS(mm/s)	1.34	1.28	1.23	1.18	1.13	1.11	
QS(mm/s)	1.87	2.03	2.36	2.18	2.13	1.95	
Field(KOe)	213	105					Fe2+
Omega(degree)	55	47					
Width(mm/s)	0.30*	0.30*	0.79	0.33	0.32	0.32	
Area (%)	17	18	35	44	44	46	
CS(mm/s)	1.40	1.19	1.21				
QS(mm/s)	2.46	2.23	2.11				

This is the peer-reviewed, final accepted version for American Mineralogist, published by the Mineralogical Society of America.
The published version is subject to change. Cite as Authors (Year) Title. American Mineralogist, in press.
DOI: https://doi.org/10.2138/am-2021-7851. http://www.minsocam.org/

Field(KOe)	93	192	49				Fe2+
Omega(degree)	45	52	56				
Width(mm/s)	0.26*	0.30*	0.26*				
Area (%)	17	16	14				
CS(mm/s)	1.01	1.01					
QS(mm/s)	2.42	2.03					
Field(KOe)	243	426					Fe2+
Omega(degree)	60	22					
Width(mm/s)	0.26*	0.30*					
Area (%)	10	13					
CS(mm/s)	1.01	0.91					
QS(mm/s)	2.10	2.42					
Field(KOe)	460	459					Fe2+ or Fe2.5+
Omega(degree)	44	39					
Width(mm/s)	0.30*	0.30*					
Area (%)	12	11					
CS(mm/s)	0.92	0.63	0.83	0.79	0.79	0.72	

QS(mm/s)	1.64	1.77	1.42	1.65	1.67	1.60	
Field(KOe)	433	262	335				Fe2.5+
Omega(degree)	13	62	10				
Width(mm/s)	0.30*	0.30*	0.30*	0.26*	0.26*	0.26*	
Area (%)	14	9	14	9	7	7	
CS(mm/s)			0.70	0.70	0.70	0.54	
QS(mm/s)			1.21	1.17	1.04	1.14	
Field(KOe)			376				Fe2.5+
Omega(degree)			38				
Width(mm/s)			0.26*	0.26*	0.26*	0.26*	
Area (%)			13	10	9	5	
CS(mm/s)				1.16	1.17	1.21	
QS(mm/s)				0.60	0.66	0.81	
Width(mm/s)				0.26*	0.26*	0.26*	Looks like ilmenite
Area (%)				9	9	7	
CS(mm/s)			0.54	0.60	0.55	0.49	

QS(mm/s)			0.69	0.77	0.86	0.89	
Field(KOe)			313				Fe3+
Width(mm/s)			0.26*	0.33	0.33	0.27	
Area (%)			13	11	15	20	
CS(mm/s)	0.49	0.64					
QS(mm/s)	0.31	-0.37					
Field(KOe)	500	479					oxide?
Width(mm/s)	0.30*	0.30*					
Area (%)	10	7					
CS(mm/s)	0.45	0.48					
QS(mm/s)	0.17	0.22					oxide?
Field(KOe)	481	489					
Width(mm/s)	0.30*	0.40*					
Area (%)	12	16					
CS(mm/s)			0.44	0.44			
QS(mm/s)			0.32	0.23			
Field(KOe)			544	543			hematite

This is the peer-reviewed, final accepted version for American Mineralogist, published by the Mineralogical Society of America.
The published version is subject to change. Cite as Authors (Year) Title. American Mineralogist, in press.
DOI: https://doi.org/10.2138/am-2021-7851. http://www.minsocam.org/

Width(mm/s)			0.35	0.26*			
Area (%)			5	4			
CS(mm/s)	0.53	0.49	0.47	0.46	0.41	0.37	
QS(mm/s)	-0.03	-0.03	-0.08	-0.06	-0.09	-0.21	
Field(KOe)	541	541	532	530	528	518	hematite
Width(mm/s)	0.30	0.30*	0.30*	0.42	0.40*	0.29	
Area (%)	9	12	6	11	15	13	
chi squared	18.4	19.5	5.2	0.9	2.4	0.8	

This is the peer-reviewed, final accepted version for American Mineralogist, published by the Mineralogical Society of America.
The published version is subject to change. Cite as Authors (Year) Title. American Mineralogist, in press.
DOI: https://doi.org/10.2138/am-2021-7851. http://www.minsocam.org/

729

730

731

732

Table 5a. Calculations needed to compare SREF and Mössbauer site assignments

SREF values as written			
		90K Fe^{2+}	90K Fe^{3+}
	Fe1	93	7
	Fe2	58	42
	Fe3	90	10
	Fe4	34	66
SREF values recast as % of Total Fe			
	Fe1	16	1
	Fe2	10	7
	Fe3	15	2
	Fe4	6	11
Mössbauer site assignments			
D1	Fe1 and Fe3	**39.3**	**0.0**
D2	Fe2 and Fe4	**15.7**	**0.0**
D3	Fe2 and Fe4	0	14.6
D4	Fe1 and Fe3	**7.9**	**7.9**
D5	Fe2 and Fe4	**7.3**	**7.3**

733

734

This is the peer-reviewed, final accepted version for American Mineralogist, published by the Mineralogical Society of America.
The published version is subject to change. Cite as Authors (Year) Title. American Mineralogist, in press.
DOI: https://doi.org/10.2138/am-2021-7851. http://www.minsocam.org/

735

736

Table 5b. Comparison of site assignments from literature and this study

	Douvalis et al. (2002) Assignments		This study Revised Assignment		This study Recast as %Fe (Table 5)	
	Mössbauer 116K	Mössbauer 116K	Mössbauer 80K	Mössbauer 80K	SREF 90K	SREF 90K
	$\%Fe^{2+}$	$\%Fe^{3+}$	$\%Fe^{2+}$	$\%Fe^{3+}$	$\%Fe^{2+}$	$\%Fe^{3+}$
Fe 1	17	0	½×(39.3+7.9) = 23.6	½×(0+7.9) = 3.9	16	1
Fe 2	½×(8+8.5) = 8.3	½×(17+8+8.5) = 16.7	½×(15.7+0+7.3) = 11.5	½×(0+14.6+7.3) = 11	10	7
Fe 3	½×(8+8.5) = 8.3	½×(17+8+8.5) = 16.7	½×(39.3+7.9) = 23.6	½×(0+7.9) = 3.9	15	2
Fe 4	33	0	½×(15.7+0+7.3) = 11.5	½×(0+14.6+7.3) = 11	6	11

737

738

739

740

741

742
743

744

745
746
747
748

This is the peer-reviewed, final accepted version for American Mineralogist, published by the Mineralogical Society of America.
The published version is subject to change. Cite as Authors (Year) Title. American Mineralogist, in press.
DOI: https://doi.org/10.2138/am-2021-7851. http://www.minsocam.org/

(FOR DEPOSIT)

Appendix 1. Parameters and Results of Mössbauer Study

Fits to the first four spectra are given in Table 4. The Mössbauer separate was found to include several impurities; as a result of these impurities, the 4K spectrum was too complex to be deconvolved into component peaks in the manner used by Douvalis et al. (2002). Fits to low-temperature, magnetically split distributions of Fe^{2+} require the use of parameters *omega* and *psi*, which indicate the orientation of the EFG with respect to the magnetic field at the nucleus, and through the parameter *eta*, which relates to the asymmetry of the EFG. Although the fitting program used here does have terms that allow for the variation of these parameters, the addition of spectral contributions from the impurities in this sample made the resultant models extremely complicated and highly non-unique. Thus fits are only given for the 295, 220, 150, and 80 K spectra.

The present fitting results are directly comparable to those obtained by Douvalis et al. (2002), as seen in Table 4a; in particular, values for IS (*isomer shift*) are strikingly similar. Values for QS are slightly different, as expected in a naturally-occurring sample with extensive cation substitution. Moreover, as noted by Douvalis et al. (2002), QS is affected by charge symmetry, anisotropic covalency, and spin–orbit coupling, all of which may be affected by the cation substitutions present in the natural sample.

Although the fit parameters obtained on our samples are similar to those of previous workers, the fact that this study has independent confirmation of Fe site assignments from SREF requires some corrections to previous workers' interpretations, which were made without that benefit. Table 4a also provides site assignments corresponding to the various Mössbauer features. Douvalis et al. (2002) assigned the designations D1 (for doublet 1) through D5 (doublet

774 5) to these features. D1 and D2 are assigned to Fe^{2+} in the Fe1 and Fe3 sites, respectively, and
775 D3, D4, and D5 represent combinations of Fe^{2+} and Fe^{3+} in the Fe2 and Fe4 sites. Fe3 and Fe4 in
776 the original Douvalis work have been switched to Fe4 and Fe3, respectively, in Table 4a to
777 match the standard site notation adopted from Swinnea and Steinfink (1983). The high IS of D3
778 might suggest that although it is mostly Fe^{3+}, though there is also some Fe^{2+} character that cannot
779 be resolved as a separate doublet. Moreover, the features D4 and D5 cannot be assigned to
780 specific sites because they represent delocalized electrons: thus their areas are average valence
781 states of Fe in adjacent sites. This sharing of electrons is facilitated by the much smaller distance
782 between Fe cations in the adjacent Fe2 and Fe4 sites (2.7835 Å at 295 K; Table 7) compared to
783 the cation-cation distances for all other adjacent Fe-pairs, which range from ~ 3.07 Å to 3.38 Å.
784 However, the assignments of Douvalis et al. (2002) are inconsistent with our site
785 occupancies known from SREF. Tables 5a and 5b use the results from ca. 100 K to reconcile
786 them with the Fe distributions seen in the Mössbauer results. To make this comparison, the site
787 occupancies determined by structure refinement (Tables 5a and 5b) are recast as percentages of
788 total Fe considering site multiplicity, rendering them directly comparable to Mössbauer results
789 (rightmost two columns of Table 5b). If the assignments by Douvalis et al. (2002) are strictly
790 applied, the 39% area for D1 overfills the Fe1 site, so this area is distributed between Fe1 and
791 Fe3, which are symmetrically equivalent and thus likely to be indistinguishable by Mössbauer.
792 Similarly, Douvalis et al. (2002) assign their D2 to Fe4, but that peak area is too large to be
793 solely Fe4, and this is likely shared by Fe2 and Fe4, again symmetrically equivalent sites. Their
794 D3, which is primarily Fe^{3+}, was thought to be distributed between Fe2 and Fe3 sites but SREF
795 finds Fe^{3+} in all the sites, so that is likely an oversimplification. Ultimately there is no *a priori*
796 way to assign a distribution of delocalized charges to a specific site.

This is the peer-reviewed, final accepted version for American Mineralogist, published by the Mineralogical Society of America.
The published version is subject to change. Cite as Authors (Year) Title. American Mineralogist, in press.
DOI: https://doi.org/10.2138/am-2021-7851. http://www.minsocam.org/

797 Tables 5a and 5b give the assignments that best reconcile the Mössbauer features with
798 SREF for this sample. Table 5a shows how the SREF site occupancies are recast to doublet areas
799 given for the 90K Fe^{2+} and Fe^{3+} features, with the Fe in D4 and D5 split between Fe^{2+} and Fe^{3+}.
800 Table 5b shows the calculations and resultant values for assigning these doublets to specific sites
801 that come closest to agreeing with SREF results. The inability to distinguish between Fe1 and
802 Fe3 (similarly Fe2 and Fe4) is not surprising as the sites comprising each pair are so similar.
803
804
805
806
807

This is the peer-reviewed, final accepted version for American Mineralogist, published by the Mineralogical Society of America.
The published version is subject to change. Cite as Authors (Year) Title. American Mineralogist, in press.
DOI: https://doi.org/10.2138/am-2021-7851. http://www.minsocam.org/

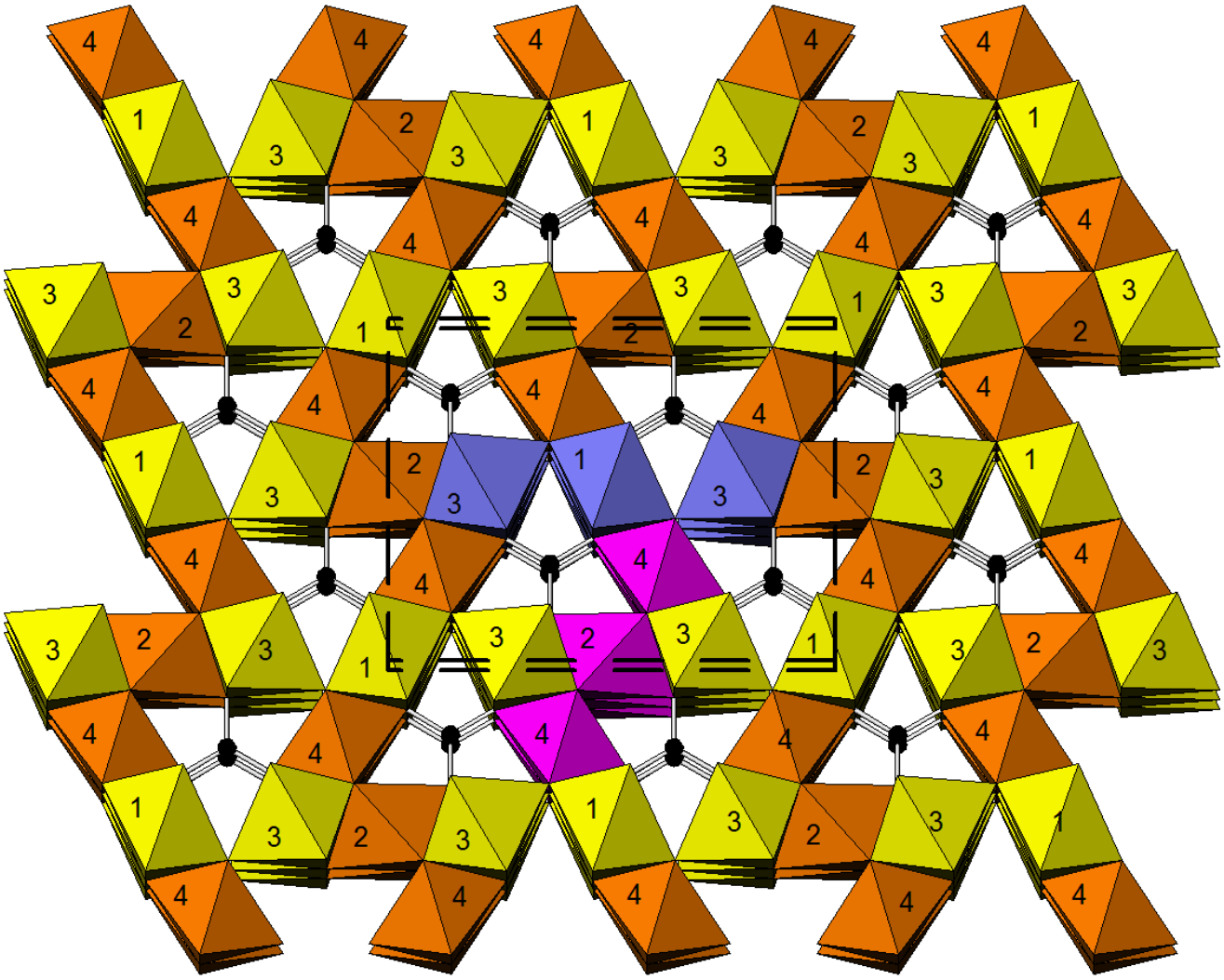
4
1
3
2
3
4
4
3
2
3
1
4
4
1
3
2
3
4
4
3
2
3
1
4
4
1
3
2
3
4
4
3
2
3
1
4

This is the peer-reviewed, final accepted version for American Mineralogist, published by the Mineralogical Society of America.
The published version is subject to change. Cite as Authors (Year) Title. American Mineralogist, in press.
DOI: https://doi.org/10.2138/am-2021-7851. http://www.minsocam.org/